Possibility of a metastable state for a transition-metal impurity in semiconductor

P. Dahan and V. Fleurov
Beverly and Raymond Sackler Faculty of Exact Sciences, School of Physics and Astronomy, Tel Aviv University, Tel Aviv 69978, Israel
(Received 20 November 1995)

A transition-metal impurity in a semiconductor can be shifted from its high symmetry substitutional position due to the Jahn-Teller interaction. An interplay of the spin-orbit and Jahn-Teller interactions may lead to a double-well potential for such an impurity in the configuration coordinates. One of these new states can be metastable and characterized by extremely long relaxation time especially at low temperatures. This allows us to explain the observation of the line complementing the intracenter transition line to the forbidden energy gap both in the luminescence and in the photoluminescence excitaton spectra. Various other puzzling experimental observations are discussed and explained on the basis of this mechanism. [S0163-1829(96)07919-2]

I. INTRODUCTION

It was originally shown by Landau[1] that states of electrons trapped by a lattice may be more favorable energetically than the Bloch band states, provided the electron-phonon interaction is strong enough. The concept of a self-trapped state actually deals with the autolocalization of free and weakly bound particles. Such states were investigated in detail by Rashba[2] for electronic excitons coupled to lattice vibrations in molecular crystals (for a review see Ref. 3).

There is a potential barrier that usually separates the free and self-trapped excitons. The barrier appears due to a short-range electron-phonon interaction provided that the coupling constant of the latter exceeds a critical value. A detailed analysis of the potential barrier created due to the interaction with the continuum of phonon modes was carried out by Toyozawa[4] who minimized the total energy by using a properly chosen variational wave function. Another way to characterize the potential barrier for excitons was proposed by Sumi.[5] The problem was treated in a linear approximation separately for two cases, with and without electron-phonon interaction. Then the results of both considerations were presented in configurational coordinates, and the intersection surface was used to obtain the potential barrier and its location in real space.

All these models deal with periodic systems and consider a possible localization of otherwise extended particles. A strong enough electron-phonon interaction may also influence the state of a defect in a crystal and may lead to creating additional minima in the configuration coordinates of the impurity and as a result to anomalously long relaxation times. This type of approach was pursued by several authors in lead-tin chalcogenides doped by normal-metal impurities.[6–8]

Here we are going to consider the behavior of a transition-metal impurity atom that occupies a substitutional position in the semiconductor lattice and study how the electron-phonon interaction can influence the location of this atom. Normally, a substitutional impurity atom resides in the highly symmetric position of the substituted host atom. However, the degeneracy of the d electron state typical for transition metals can cause a Jahn-Teller distortion and shift the atom to a lower symmetry position. As will be shown below a strong enough Jahn-Teller interaction together with the spin-orbit coupling may result not only in a simple shift, but also in a situation when the original high symmetry position is separated by a potential barrier from the lower symmetry position. Hence, the configurational potential for the impurity atom may have more than one minimum, meaning an appearance of metastable states.

Standard solutions of problems involving both Jahn-Teller and spin-orbit interactions are usually found assuming one of these perturbations to be small as compared to the other. Such approximations enable one to diagonalize the system with respect to the larger interaction and to account for the smaller one as a perturbation. We, however, are going to consider both interactions on an equal footing while diagonalizing the problem.

There is a lot of discussion in the literature concerning the roles of these two interactions and the mechanisms that can change their magnitudes. Two mechanisms can be responsible for orbital reduction factors in matrix elements of the spin-orbit interaction.[9] The Ham effect[10] appearing in the case of a strong electron-vibron interaction is one of these mechanisms. It may result in an exponentially strong reduction of the linear spin-orbit contribution, whereas the second-order term may remain finite and in some times even larger than the first-order term. The case of the Cu(d^9) impurities is discussed in Ref. 11 (for a more general review see Ref. 12). The second mechanism is the covalency effect resulting from the electron delocalization due to a spread of the electron wave function over the neighboring atoms.[9,13–17]

It is usually assumed that the magnitude of the $^2T_2$ ground-state splitting, caused by the spin-orbit interaction, is strongly reduced due to the electron-vibron interaction. However, the authors of Ref. 14 consider an intermediate Jahn-Teller interaction and introduce also a covalency reduction in order to explain the small g value observed for the Cu($^2T_2$) ground state. In order to explain simultaneously the $^2T_2$ splitting and the value of $g(\Gamma_7)$ Ref. 11 had to consider a strong Jahn-Teller interaction and an admixture of the excited state ^2E. Reference 18 claims that, in contrast to what has been assumed above, the quenching of the g factor of the Cu^{2+} doped ZnS can be understood only if a weak Jahn-Teller coupling is assumed and if the interaction is with lo-

 © 1996 The American Physical Society

calized vibrational modes. A special emphasis on the role of the hybridization of the impurity *d* electron with ligand states was discussed in Ref. 19, which showed that this mechanism leads to an increase of the Jahn-Teller coupling.

All this actually means that the question of what is the ratio of the magnitudes of the two mechanisms is still open and that various possibilities exist. There is not enough experimental and theoretical information to allow one to make a specific choice. That is why we are not going to make such a choice either. Our aim is to consider what happens if different ratios of the Jahn-Teller and spin-orbit couplings take place, and what is the role of the covalency in this effect.

This paper presents a mechanism that may possibly lead to a creation of a metastable state for the transition-metal impurity. This results from a competition between the Jahn-Teller and spin-orbit interactions enhanced by the covalent hybridization of the impurity *d* electrons with the band electrons. The mechanism will be considered in detail at the example of the Cu impurity in ZnS. This system presents a special interest for us because the possibility that an ^2E excited Cu impurity is in a metastable state (in the configuration coordinates) may imply anomalously long relaxation times at low temperatures, which seem to be necessary for a proper interpretation of various experimental observations.

Some of these are mentioned below. The decay time of the infrared luminescence in ZnS:Cu (Ref. 20) decreases with decreasing temperature instead of reaching a plateau at temperatures below 80 K as is expected according to the configuration mixing mechanism for the electronic transition probabilities of $3d$ ions.[21] This may be understood if relaxation proceeds from a long living metastable state.

The assumption of a long relaxation time from the metastable state of the impurity allows one also to solve the problem of the sum rule found in the spectra of ZnS:Cu and CdS:Cu.[22,23] These authors observed a line in the blue part of the spectrum that complements the red line, corresponding to an impurity intracenter transition, just to the forbidden energy gap. The model proposed in the previous papers of the current authors[24,25] presents a consistent explanation of this sum rule in the *luminescence* spectra of these systems. However, the same model applied to the photoluminescence *excitation* requires the electronically excited $\mathrm{Cu}^{(2+)}(^2E)$ as the initial state of the process. This would have been hardly possible due to a negligibly small occupation of this state at thermal equilibrium, unless there was a very long relaxation time in the metastable state.

Two additional experimental observations, showing an intimate connection between the infrared and blue lines, can be interpreted assuming long-living electronically excited states of $\mathrm{Cu}(^2E)$. These will be discussed at the end of this paper.

II. MODEL

A *d* impurity in a semiconductor can be described by means of the Hamiltonian

$$H_e=\hat{T}+V_d(\mathbf{r}-\mathbf{R}_0)+U'(\mathbf{r}-\mathbf{R}_0)+U_1\{\Delta\rho(\mathbf{r})\}+H_I, \tag{1}$$

where $\hat{T}$ is the electron kinetic energy operator, $V_d(\mathbf{r}-\mathbf{R}_0)$ is the substitutional impurity potential at the site $\mathbf{R}_0$, and $U'(\mathbf{r},\{\mathbf{R}_i\})$ is the lattice potential acting on the impurity electron and depending on the equilibrium positions, $\{\mathbf{R}_i\}$, of the lattice atoms, $U\{\Delta\rho(\mathbf{r})\}$ is the potential due to the valence electrons disturbed by the impurity.

The perturbation Hamiltonian

$$H_I=V^{\mathrm{SO}}+V^{\mathrm{JT}} \tag{2}$$

includes two interactions to be discussed below. The first one is the spin-orbit interaction represented in the form

$$V^{\mathrm{SO}}=\frac{\hbar}{4m^2c^2}[\nabla V_d,\hat{\mathbf{p}}]\hat{\boldsymbol{\sigma}}, \tag{3}$$

where $\hat{\mathbf{p}}$ is the electron momentum operator and $\hat{\boldsymbol{\sigma}}$ is the vector of the Pauli matrices.

The second perturbation is the Jahn-Teller interaction, linearized with respect to the normal vibronic coordinates $Q_{\Gamma\mu}$, which in the matrix form reads

$$V^{\mathrm{JT}}=\sum_{\Gamma''\mu''} V_{\Gamma''}Q_{\Gamma''\mu''}\rho^{\Gamma''\mu''}_{\Gamma\mu,\Gamma'\mu'}. \tag{4}$$

V_Γ is the electron-lattice coupling coefficient for the Γ irreducible representation for lattice distortions (point group T_d is implied throughout this paper). $\rho^{\Gamma''\mu''}_{\Gamma\mu,\Gamma'\mu'}$ is the tensor described in the Appendix whose upper indices relate to lattice coordinates while the lower indices relate to the electrons.

The problem is addressed within the model of resonant scattering of electrons by transition-metal impurities in semiconductors whose detailed account is presented in Ref. 17. Single electron impurity functions are expanded using the set of functions $\{\tilde{\psi}_{\mathbf{k}a},\psi_{\gamma\mu}\}$, which includes the wave functions $\psi_{\gamma\mu}$ of the atomic *d* electrons in the local crystal field and the Bloch functions

$$\tilde{\psi}_{\mathbf{k}a}=\psi_{\mathbf{k}a}-\sum_{\gamma\mu}\langle\gamma\mu|\mathbf{k}a\rangle\psi_{\gamma\mu},$$

orthogonalized to the *d*-electron wave functions. The electron wave function in the deep level is looked for in the form

$$\psi_{i\gamma\mu}=F^{\gamma\mu}_d\psi_{\gamma\mu}+\sum_{\mathbf{k}a}F^{\gamma\mu}_{\mathbf{k}a}\tilde{\psi}_{\mathbf{k}a}. \tag{5}$$

This function transforms as the μth row of the irreducible representation γ and the problem is now to find the set of the coefficients $\{F^{\gamma\mu}_{\mathbf{k}a},F^{\gamma\mu}_d\}$.

These coefficients are found from the condition that the wave function (5) is an eigenfunction of the Hamiltonian (1), which can be represented in the following matrix form (see, e.g., Ref. 26)

$$\mathbf{M\Phi}\equiv\begin{pmatrix}\mathbf{B} & -\mathbf{V}^T\\ -\mathbf{V} & \mathbf{D}\end{pmatrix}\begin{pmatrix}\mathbf{b}\\ \mathbf{d}\end{pmatrix}=0, \tag{6}$$

where

$$(\mathbf{b},\mathbf{d})=(F^{\gamma\mu}_{\mathbf{k}a},F^{\gamma\mu}_d)$$

and T denotes the transposition of the matrix. Other definitions are as follows:

$$B_{\mathbf{k}a,\mathbf{k}'a'}=(E-\varepsilon_{\mathbf{k}a})\,\delta_{\mathbf{k}\mathbf{k}'}\,\delta_{aa'}-\sum_{\mathbf{k}'a'}X_{\mathbf{k}a,\mathbf{k}'a'}, \tag{7}$$

$$D_{\gamma\mu,\gamma'\mu'}=(E-\varepsilon_{\gamma})\,\delta_{\gamma\gamma'}\,\delta_{\mu\mu'}-\langle\gamma\mu|V^{\mathrm{SO}}+V^{\mathrm{JT}}|\gamma'\mu'\rangle, \tag{8}$$

$$V=\sum_{\mathbf{k}'a'}\langle\gamma\mu|W+V^{\mathrm{SO}}+V^{\mathrm{JT}}|\tilde{\mathbf{k}}'a'\rangle; \tag{9}$$

ε_{γ} is the energy of the d level in the local crystal field W; the matrix element

$$X_{\mathbf{k}a,\mathbf{k}'a'}=U^{(s)}_{\mathbf{k}a,\mathbf{k}'a'}+V^{\mathrm{SO}}_{\mathbf{k}a,\mathbf{k}'a'}+V^{\mathrm{JT}}_{\mathbf{k}a,\mathbf{k}'a'} \tag{10}$$

incorporates contributions of the potential part of the impurity scattering, spin-orbit coupling, and Jahn-Teller interaction. This will be neglected in what follows as compared to the resonant scattering contribution.

The zeros of the matrix $\mathbf{M}$ can be found using the transformed matrix

$$\begin{pmatrix}\mathbf{B} & -\mathbf{V}^T\\ -\mathbf{V} & \mathbf{D}\end{pmatrix}\begin{pmatrix}\mathbf{I} & \mathbf{B}^{-1}\mathbf{V}^T\\ \mathbf{D}^{-1}\mathbf{V} & \mathbf{I}\end{pmatrix}=\begin{pmatrix}\mathbf{B}-\mathbf{V}^T\mathbf{D}^{-1}\mathbf{V} & \mathbf{0}\\ \mathbf{0} & \mathbf{D}-\mathbf{V}\mathbf{B}^{-1}\mathbf{V}^T\end{pmatrix}. \tag{11}$$

Since $\det\mathbf{M}$ becomes zero simultaneously with the determinant of the matrix in the right-hand side of Eq. (11) the latter becomes zero whenever the determinants of any of the matrices in its diagonal become zero, e.g.,

$$\det[\mathbf{D}(E)-\mathbf{V}\mathbf{B}^{-1}(E)\mathbf{V}^T]=0, \tag{12}$$

where

$$\mathbf{D}(E)=(E-\varepsilon_{\gamma})\,\delta_{\gamma\gamma'}\,\delta_{\mu\mu'}-\langle\gamma\mu|V^{\mathrm{SO}}+V^{\mathrm{JT}}|\gamma'\mu'\rangle, \tag{13}$$

$$\mathbf{V}\mathbf{B}^{-1}\mathbf{V}^T=\sum_{\mathbf{k}a}\frac{\langle\gamma\mu|W+V^{\mathrm{SO}}+V^{\mathrm{JT}}|\mathbf{k}a\rangle\langle\mathbf{k}a|W+V^{\mathrm{SO}}+V^{\mathrm{JT}}|\gamma'\mu'\rangle}{E-\varepsilon_{\mathbf{k}a}}. \tag{14}$$

The determinant (12) can be written in the form

$$\det\{[E-\varepsilon_{\gamma}-M_{\gamma}(E)]\,\delta_{\gamma\gamma'}\,\delta_{\mu\mu'}-M_{\gamma\mu,\gamma'\mu'}\}=0, \tag{15}$$

where

$$M_{\gamma}\delta_{\gamma\gamma'}\,\delta_{\mu\mu'}=\langle\gamma\mu|W\mathbf{G}W|\gamma\mu\rangle,$$

$$\mathbf{G}=\sum_{\mathbf{k}a}\frac{|\mathbf{k}a\rangle\langle\mathbf{k}a|}{E-\varepsilon_{\mathbf{k}a}},$$

$$M_{\gamma\mu,\gamma'\mu'}=V^{\mathrm{SO}}_{\gamma\gamma'}+V^{\mathrm{JT}}_{\gamma\gamma'}+M^{\mathrm{SO}}_{\gamma\gamma'}+M^{\mathrm{SO,JT}}_{\gamma\gamma'}+M^{\mathrm{JT}}_{\gamma\gamma'}+M^{\mathrm{SO,SO}}_{\gamma\gamma'} \tag{16}$$

and

$$M^{\mathrm{SO}}_{\gamma\gamma'}=\langle\gamma\mu|W\mathbf{G}V^{\mathrm{SO}}|\gamma'\mu'\rangle+\langle\gamma\mu|V^{\mathrm{SO}}\mathbf{G}W|\gamma'\mu'\rangle,$$

$$M^{\mathrm{SO,JT}}_{\gamma\gamma'}=\langle\gamma\mu|V^{\mathrm{SO}}\mathbf{G}V^{\mathrm{JT}}|\gamma'\mu'\rangle+\langle\gamma\mu|V^{\mathrm{JT}}\mathbf{G}V^{\mathrm{SO}}|\gamma'\mu'\rangle,$$

$$M^{JT}_{\gamma\gamma'}=\langle\gamma\mu|W\mathbf{G}V^{\mathrm{JT}}|\gamma'\mu'\rangle+\langle\gamma\mu|V^{\mathrm{JT}}\mathbf{G}W|\gamma'\mu'\rangle, \tag{17}$$

$$M^{\mathrm{SO,SO}}_{\gamma\gamma'}=\langle\gamma\mu|V^{\mathrm{SO}}\mathbf{G}V^{\mathrm{SO}}|\gamma'\mu'\rangle.$$

Without the spin-orbit and Jahn-Teller interactions Eq. (15) takes the form

$$\varepsilon_{i\gamma}=\varepsilon_{\gamma}+M_{\gamma}(\varepsilon_{i\gamma}),$$

so that its solutions yield positions, ε_{it} and ε_{ie}, of the d levels. The spin-orbit and Jahn-Teller interactions result in off-diagonal terms in the matrix (16) and, hence, in an additional splitting of the levels according to the irreducible representations of the double T_d group. The Jahn-Teller interaction introduces a configuration coordinate dependence.

It is important to emphasize that both these interactions interfere also with the covalent hybridization, which is reflected by the third to sixth terms in the right-hand side of Eq. (16). One can see that while two second-order hybridization contributions are kept, the third one, $M^{\mathrm{JT,JT}}_{\gamma\gamma'}$ is omitted. The latter may be of importance when dealing with the γ_7 state, which is not considered in this paper. As for the other second-order terms they are necessary for a proper calculation of the configuration diagrams to be done in the next section.

III. METASTABLE STATES AT THE EXAMPLE OF THE Cu IMPURITY

In order to be more specific, we consider here the Cu impurity in a wurzite type II-VI semiconductor for which much experimental information is available. The d shell of the impurity has nine electrons (or one d hole) and may have two electronic configurations, ${}^2T_2(d^9)$ and ${}^2E(d^9)$, in a tetrahedral surrounding. The hole representation is more convenient in this case since it allows us to use single-electron wave functions and to avoid complications of the multielectron configurations of the d shell. The double group T_d contains two irreducible representations, γ_8 and γ_7, which are of interest in the context of our problem and correspond to the $j=\frac{3}{2}$ and $j=\frac{1}{2}$ electronic angular moments, respectively. The sixfold degenerate level, t_2, of the hole in the d shell of the Cu impurity is split by the spin-orbit coupling into two levels corresponding to these two representations, as for the e state it is described by means of the γ_8 representation of

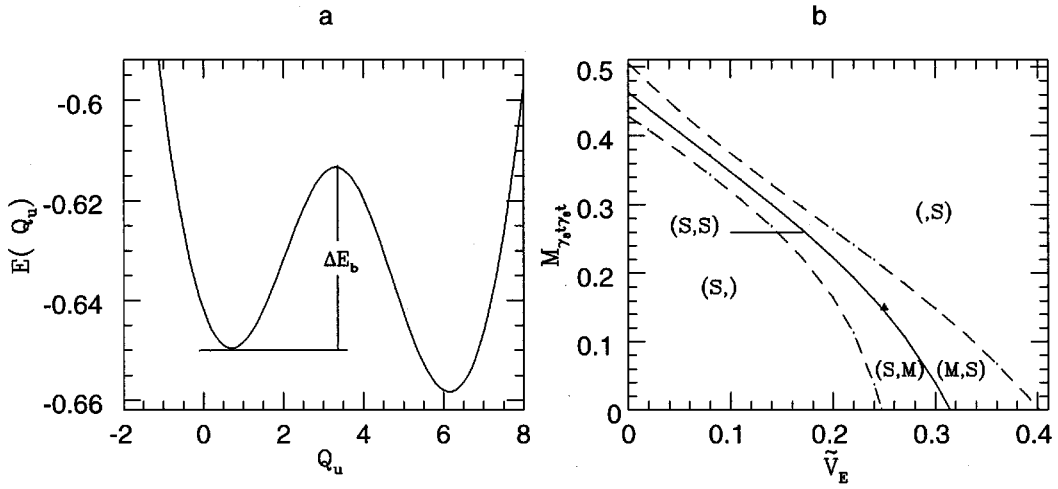

FIG. 1. The graph (a) shows the energy $E(Q_u)$ of the electronically excited Cu(^2E) state vs the configuration coordinate Q_u. The crystal field splitting is chosen to be $Dq=0.094$ eV, the spin-orbit coupling is characterized by the parameters $\tilde{\lambda}_t=0.7$ eV and $\tilde{\lambda}_{te}=0.48$. The hybridization contributions are $M_{\gamma_8 t_2 \gamma_8 t_2}=0.15$ eV, $M_{te}=0.3$ eV, and $M_{\gamma_8 t_2 \gamma_8 e}=0.13$ eV. Then the d level splitting renormalized by the hybridization becomes $\Delta E(^2E-{}^2T_2)=0.866$ eV and the double-well potential with the barrier height $\Delta E_b=0.037$ eV is obtained for the effective Jahn-Teller interaction $\tilde{V}_E=0.25$ eV. $\hbar\omega=0.05$ eV is the frequency of oscillations along the Jahn-Teller distortion coordinate, which is kept the same for all figures in this paper. The diagram (b) shows what types of the potential can be obtained for various values of the quantities $\tilde{V}_E$ and $M_{\gamma_8 t_2 \gamma_8 t_2}$. The potential of the graph (a) is shown by the full triangle. S stands for the lower (stable) whereas M stands for the higher (metastable) minimum. The potentials on the solid line have wells of equal depths, while the dashed lines separate the double-well and single-well areas.

the double group. As a result it is convenient, in what follows, to use the basis $\{\psi_{\gamma_8 t_2 \mu}, \psi_{\gamma_8 e \mu}, \psi_{\gamma_7 t_2 \mu}\}$, where μ classifies the functions within each irreducible representation.

Using this basis and assuming that the Jahn-Teller distortion is along the u normal mode of the E representation (for a definition see, e.g., Ref. 27), Eq. (16) becomes a rather cumbersome 10×10 matrix whose detailed description is presented in the Appendix. Hopefully, this matrix contains many zero elements, which allows one to carry out the calculations until a rather transparent result is obtained.

The principal idea of how a metastable state in the configurational coordinate space can appear is demonstrated by means of the secular equation

$$[E-\varepsilon'_{it}(\gamma_8,\pm\tfrac{1}{2})][E-\varepsilon'_{ie}(\gamma_{8,}\pm\tfrac{1}{2})]-|\chi_{te}(\gamma_{8,}\pm\tfrac{1}{2})|^2=0$$

obtained by equating the determinant of the matrix (A14) to zero. Solving this quadratic equation one gets

$$E^{(\pm)}(\mp\tfrac{1}{2})=\tfrac{1}{2}(\varepsilon'_{it}+\varepsilon'_{ie})\pm[\tfrac{1}{4}(\Delta_{CF}^{\rm cov}+\tfrac{1}{2}\tilde{\lambda}_t-\alpha_1 Q_u)^2 + (\sqrt{\tfrac{3}{2}}\tilde{\lambda}_{te}-\alpha_2 Q_u)^2+M_{te}^2]^{1/2} \quad (18)$$

where

$$\alpha_1=\frac{M_{\gamma_8 t_2 \gamma_8 t_2}+(\sqrt{3}-1)\tilde{V}}{\sqrt{6}},$$

$$\alpha_2=\frac{\sqrt{3}+1}{2}M_{\gamma_8 t_2 \gamma_8 e}.$$

and

$$\Delta_{CF}^{\rm cov}=\Delta_{CF}^0+M_e(E_{ie})-M_{t_2}(E_{it_2}).$$

The corresponding impurity wave functions are

$$\psi_{it}^{(+)}(\mp\tfrac{1}{2})=\frac{1}{\sqrt{1+x^2}}[\psi_{i\gamma_8 t}(\mp\tfrac{1}{2})+|x|e^{-i\theta}\psi_{i\gamma_8 e}(\mp\tfrac{1}{2})],$$

$$\psi_{ie}^{(-)}(\mp\tfrac{1}{2})=\frac{1}{\sqrt{1+x^2}}[\psi_{i\gamma_8 e}(\mp\tfrac{1}{2})-|x|e^{i\theta}\psi_{i\gamma_8 t}(\mp\tfrac{1}{2})], \quad (19)$$

where

$$x=\sqrt{\frac{1}{4}\left(\frac{\Delta'_{CF}}{\chi}\right)^2+1}-\frac{1}{2}\frac{\Delta'_{CF}}{\chi},$$

$$\tan\theta(\mp\tfrac{1}{2})=\frac{\sqrt{\frac{3}{2}}\tilde{\lambda}_{te}\mp\alpha_2 Q_u}{M_{te}}, \quad (20)$$

and

$$\Delta'_{CF}=\Delta_{CF}^{\rm cov}+\tfrac{1}{2}\tilde{\lambda}_t-\alpha_1 Q_u. \quad (21)$$

Equations (18) and (19) describe two electron levels resulting from the states $\{\gamma_8, t(\pm\frac{1}{2})\}$ and $\{\gamma_8, e(\pm\frac{1}{2})\}$ mixed due to the Jahn-Teller and spin-orbit interactions. The total energy of each of these levels as a function of the configuration coordinate Q_u is obtained by adding the lattice energy $\frac{1}{2}Q_u^2$ in Eq. (18). Then the energies (18) become nonlinear and not necessarily monotonous functions of the configuration coordinate Q_u. Therefore, they, in principle, have more than one minimum.

Now we have an equation that, depending on the parameters, enables us to receive various shapes of the adiabatic

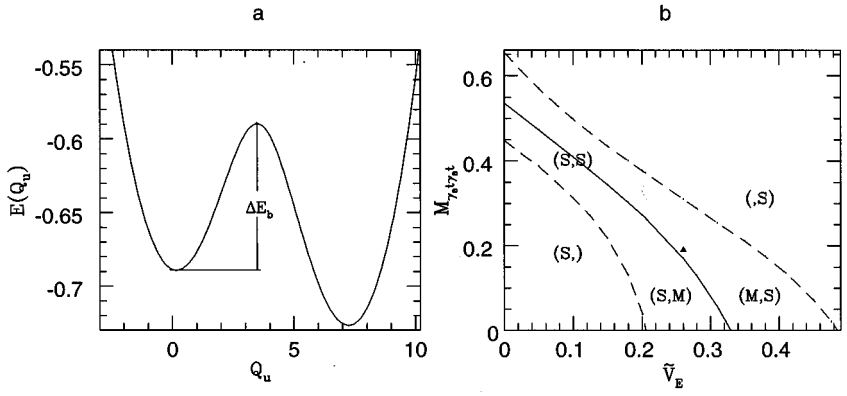

FIG. 2. The same as in Fig. 1 but with the parameters $Dq=0.092$ eV, $\tilde{\lambda}_t=0.8$ eV, $\tilde{\lambda}_{te}=0.58$ eV, $M_{\gamma_8 t_2 \gamma_8 t_2}=0.19$ eV, $M_{te}=0.25$ eV, and $M_{\gamma_8 t_2 \gamma_8 e}=0.1457$ eV. The splitting becomes $\Delta E(^2E-{}^2T_2)=0.868$ eV and the barrier height $\Delta E_b=0.1$ eV is obtained for $\tilde{V}_E=0.26$ eV.

potential. Three examples are shown in Figs. 1(a)–3(a). These potentials are characterized by two minima in which the impurity can dwell. Disregarding the possibility of an electronic transition, the lower of these two minima can be assumed to be a stable state of the impurity, while the higher one provides a metastable state. A transition between these two states in the configuration space requires an activation or tunneling transition through the barrier separating these two minima.

These figures present energy curves for various possible combinations of the parameters which fit the Cu(^2E)-Cu($^2T_2$) energy splitting in ZnS. All three curves are double-well potentials differing by locations of their minima so that the metastable well may have positive, zero, and negative displacements, respectively. The choice of the parameters is done in a such a way as to be possibly close to the known experimental value of the splitting $\Delta E(^2E-{}^2T_2)=0.868$ eV. We see that a double-well potential appears for really differing parameters such as $\tilde{V}_E=0.25$ eV in Fig. 1 and $\tilde{V}_E=0.054$ eV in Fig. 3. The higher minimum in Fig. 2 corresponds to the central position of the impurity atom whereas Figs. 1 and 3 exhibit this minimum in asymmetric positions with differing signs of the distortions. The $-$ sign corresponds to a local contraction, the $+$ sign corresponds to a local expansion. It is worthwhile to emphasize that the available experimental information is currently in no way sufficient to make a decision on which of the situations truly takes place.

The shape of the adiabatic potential depends on several parameters (18), therefore it can be a symmetric or an asymmetric double well or a simple single well potential. Figures 1(b)–3(b) show areas in the plane of the renormalized Jahn-Teller interaction $\tilde{V}_E$ versus the hybridization enhanced mixing, $M_{\gamma_8 t_2 \gamma_8 t_2}$, of spin-orbit and Jahn-Teller interactions (A13). Depending on the position in this plane different possibilities are realized. S stands for the stable state while M stands for the metastable state. Therefore, e.g., (S,M) denotes the area in the plane where double-well potentials can be found with the left lower well and right higher well. Each diagram (b) shows how the shape of the potential depends on two parameters [other parameters corresponding to the potential in the graph (a) of the same figure]. Double-well potentials appear only for the parameter values lying between the two dashed lines with the full line corresponding to double-well potentials with equally deep wells. In the outside area only single-well potentials are possible.

If the adiabatic potential corresponding to the electronically excited state ^2E has two minima the relaxation time from the metastable state may appear to be extremely large (minutes or even hours). As a result, an electronically excited impurity may live very long and its extremely slow relaxation can be overlooked in an experiment unless special care is taken.

Now rough estimates of the relaxation rate from the metastable state are given. This relaxation may proceed in two ways: (1) tunneling through the potential barrier and (2) a phonon stimulated overbarrier transition. At temperatures essentially lower than the barrier energy tunneling transitions control the relaxation. Then the decay rate can be estimated as

$$\frac{1}{\tau}=\omega\ \exp\left\{-\frac{1}{\hbar}\sqrt{2ME_b}\Delta R\right\}, \tag{22}$$

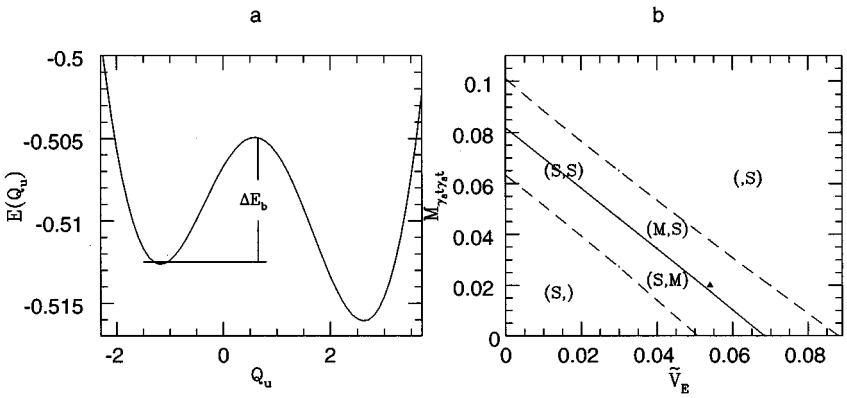

FIG. 3. The same as in Fig. 1 but with the parameters $Dq=0.089$ eV, $\tilde{\lambda}_t=0.1$ eV, $\tilde{\lambda}_{te}=0.08$ eV, $M_{\gamma_8 t_2 \gamma_8 t_2}=0.02$ eV, $M_{te}=0.1$ eV, and $M_{\gamma_8 t_2 \gamma_8 e}=0.119$ eV. The splitting becomes $\Delta E(^2E-{}^2T_2)=0.871$ eV and the barrier height $\Delta E_b=0.0075$ eV is obtained for $\tilde{V}_E=0.054$ eV.

where ω is on the order of the oscillation frequencies within potential wells, E_b and ΔR are the barrier height and width, and M is the tunneling mass, which is taken here to be close to that of the impurity. Using the dimensionless coordinate for the width of the barrier ΔQ the estimate of the decay rate (22) becomes

$$\tau = \tau_\omega \exp\left\{ \sqrt{\frac{2(\Delta Q)^2 E_b}{\hbar \omega}} \right\}. \tag{23}$$

Now substituting parameters used in Fig. 1 in Eq. (23) one gets approximately $\tau \sim \tau_\omega e^{16}$ and assuming $\tau_\omega \simeq 10^{-12}$ s the decay time can be estimated as $\tau \simeq 10^{-4}$ s. Parameters used in Fig. 2 lead us to $\tau \sim \tau_\omega e^{31}$ and to a much longer decay time $\tau \simeq 10^3$ s. As for Fig. 3 the time is much shorter, 10^{-10} s. We have here the usual situation when the theory cannot give any reliable estimates for the time of the tunneling transition due to its extreme sensitivity to the transparency of the barrier. On the other hand, these results show that the lifetime may vary by orders of magnitude within reasonable values of the parameters and in particular may be extremely large.

The possibility of a double-well potential in the electronically excited state of the impurity and, hence, a very long lifetime leads to interesting conclusions, which can be verified experimentally and help us to interpret available experimental data. A discussion of some available experimental data and their comparison with predictions of our model is presented in the next section.

IV. EXPERIMENTAL OBSERVATIONS

A. Temperature dependence of the relaxation time

Temperature dependence of the relaxation time τ of electronically excited d impurities in II-VI crystals is an important characteristic that can be studied by measuring the decay of the infrared luminescence in these systems. The experiments[21] show a temperature-independent lifetime at low temperatures whereas above approximately 100 K the lifetime starts decreasing with increasing temperature. This type of behavior is explained by the configuration mixing mechanism[28] for the electronic transition probabilities of $3d$ ions.

The decay of the infrared luminescence due to the Cu(^2E)-Cu($^2T_2$) transitions in ZnS:Cu is also known to have the above-mentioned type of behavior. However, a precision measurement of this decay time in the very low temperature range shows a deviation from this pattern. The lifetime grows from the value of 169 to 247 ns when the temperature increases from 2 to 80 K (see, Fig. 2 in Ref. 20). This type of behavior can be explained if one assumes transitions from the electronically excited Cu(^2E) impurity, characterized by at least two minima in the configuration space, to the Cu($^2T_2$) ground state of this impurity.

The following problem is examined. We assume that the occupations of the two possible states corresponding to two minima, E_2 and E_3, of the electronically excited Cu(^2E) impurity are N_2^0 and N_3^0, respectively. Then the relaxation to the electronic ground state Cu($^2T_2$) is controlled by the equations

$$\dot{N}_3 = -N_3\beta + N_2 p_{23},$$

$$\dot{N}_2 = N_3 p_{32} - N_2 \alpha, \tag{24}$$

where $\alpha = p_{23} + p_{21}$ and $\beta = p_{32} + p_{31}$ and p_{23} and p_{32} are the probabilities of the radiationless transition between the E_2 and E_3 states, while, p_{31} and p_{21} are the corresponding transitions probabilities to the ground state E_1 and may, in principle, incorporate both radiative and radiationless transitions.

For an accurate analysis of the temperature dependence of the decay time the probability of a nonradiative transition between these two minima is to be estimated. It is clear that two different temperature dependences are expected in the low-temperature range due to tunneling through the potential barrier and another one at higher temperatures when the activation regime is reached.

Let us assume, for the sake of simplicity, that the conditions $p_{32}, p_{23} \gg p_{21}, p_{31}$ hold. If, at the time $t = 0$, the Boltzmann distribution

$$\frac{N_3^0}{N_2^0} = \frac{p_{23}}{p_{32}} = e^{-\Delta E_{32}/KT}$$

between the two electronically excited states 2 and 3 holds, then according to Ref. 29,

$$N_2(t) = N_2^0 e^{-pt},$$

$$N_3(t) = N_3^0 e^{-pt}. \tag{25}$$

Here the relaxation process is characterized by the decay rate

$$p = \frac{1}{\tau_F} = p_{21}\left(\frac{e^{\Delta E_{32}/KT}}{1 + e^{\Delta E_{32}/KT}} \right) + p_{31}\left(\frac{1}{1 + e^{\Delta E_{32}/KT}} \right). \tag{26}$$

Now assuming $p_{21} \gg p_{31}$, the experimental curve (Fig. 2 in Ref. 20) is compared with the dependence produced by equation (26). The two curves appear to be rather similar. This similarity is important evidence in favor of a metastable state in the electronically excited Cu(^2E) in ZnS.

B. Sum rule in the absorption

The possibility of a metastable state is necessary to complete our explanation[24,25] of the sum rule in the optical spectra observed in several semiconductors doped by transition-metal impurities. The model presented in these papers assumes a second-order process during which the impurity is electronically excited. It does not present any problem for the luminescence since this electronically excited state of the impurity is the final state of the process. However, observation of the same sum rule in the photoluminescence excitation spectra creates a real puzzle, since then this electronically excited state must be the initial state of the process. The question is why electronically excited impurities are available in the semiconductor.

A possible answer proposed here is that these electronically excited impurities occupy the ancillary minimum of the configuration potential (metastable state), so that the relaxation from this state appears to be extremely slow, since it is strongly hindered at low temperature by tunneling along the corresponding configuration coordinate. An effective tunneling mass of an atomic order (see estimates at the end of the

previous section) is necessarily involved. Then any external irradiation or insufficient annealing of the sample always leave a large amount of the impurity atoms in the excited metastable state. As a result there are enough electronically excited impurities ready for the process, which is inverse to the process considered in Refs. 24 and 25 and the complementary line can be also observed in the photoluminescence excitation spectra. The experiment shows that the blue line in photoluminescence excitation is observed at very low temperatures and disappears at temperatures between 25 and 30 K whereas the blue luminescence band survives until 40 K. This difference may be also connected with our mechanism but a better study is necessary to make a more reliable statement.

Here we also would like to mention two additional experimental observations whose interpretation can be provided by the scheme described in this and previous papers.[24,25] These are as follows.

(1) The intensity of the Cu blue band emission in ZnS:Cu increases if additionally an infrared light is shined onto the sample[30] (Fig. 3.8). The study of this effect was done over the range of $1.2-1.5$ μm wavelengths of the light. It has been observed that the effect of the 1.4-μm light is stronger than that of the 1.5-μm light while the 1.2-μm light has no effect on the luminescence.

It is clear that we have a direct connection between the intracenter (1.4 μm) and the blue band transitions. This behavior can be explained by taking into account both the mechanism resulting in the complementing line[24,25] and the existence of a metastable state of the electronically excited Cu(^2E) characterized by a very long relaxation time. The ultraviolet light produces electron hole pairs whose recombination via the second-order process described in Refs. 24 and 25 is accompanied by the blue light emission and leaves the excited $\mathrm{Cu}^{(+2)}(^2E)$ as the final state of the system. Such impurities may occupy a metastable state of the $\mathrm{Cu}^{(+2)}(^2E)$ impurity with a long relaxation time. The blue line emission requires the $\mathrm{Cu}^{(+2)}(^2T_2)$ ground state of the impurity to be the initial state and, hence, the electronically excited impurities do not contribute to the process. Shining the infrared light in resonance with the intracenter transition stimulates a more rapid relaxation of the long living states and results in an increase of the proportion of the Cu atoms in the $^2T_2$ ground state. As a result there are now more impurity atoms participating in the luminescence yielding the complementing blue line.

(2) Sort of an inverse situation (with respect to the previous experiment) takes place when the red band absorption spectrum is measured in samples irradiated by the blue light (Figs. 4A and 4B of Ref. 31). Such an irradiation increases the absorption by a factor of about ten. In this case the absorbed blue light (the complementing line) actually converts the atoms from the metastable ^2E state into the ground $^2T_2$ state. Thus the population of Cu atoms in the ground state increases and they give an additional contribution to the infrared absorption.

These results show an intimate connection between the infrared and blue lines that is quite obvious from the point of view of the model described in the Refs. 24 and 25 and this paper. However, it is rather early to claim that the model is really verified experimentally. More measurements specifically directed to check various consequences of the model are necessary to become sure that the model works.

V. SUMMARY

This paper proposes a microscopical mechanism allowing for the appearance of a long-living metastable state of an electronically excited d impurity center. Such a possibility appears due to an interplay of the spin-orbit and Jahn-Teller interactions enhanced by the covalency. Here the model is applied to the specific case of Cu in ZnS for which experimental data are available. However, the mechanism is general and can be of importance in other systems as well.

The impurity atom may dwell now in an adiabatic double-well potential so that its relaxation at low temperatures is associated with tunneling and may be extremely slow. This allows one to address several experimental observations, as described above, and explain the features observed.

We would like to emphasize that the mechanism leading to a double-well potential, as described in this paper, is possible, in principle, without the covalency effects. Then, however, it appears to be extremely weak and can hardly have any influence on the spectra. The covalency (hybridization of the d and Bloch states) strongly enhances the effect and the height of the barrier in the double-well potential as shown in Figs. 1–3.

We may conclude that the possibility for an impurity to occupy such a metastable state plays an important role in the optics of semiconductors doped by transition-metal impurities. It is noted also that only one specific distortion is considered here as an example demonstrating the principal possibility of the metastable state. The real Jahn-Teller distortion may be different and more complicated. It can be established only on the basis of more detailed experimental investigations, which are still to be done.

ACKNOWLEDGMENTS

The authors are deeply indebted to I. Broser, A. Hoffmann, and P. Thurian for numerous stimulating discussions of their experimental results.

APPENDIX

The first term in the matrix (16) is due to the spin-orbit interaction, which mixes only states from the irreducible representations γ_{8t_2} and γ_{8e} with coinciding indices μ. That is why the whole matrix can be easily constructed by means of a smaller matrix

$$V^{\mathrm{SO}}_{\gamma\gamma'}\delta_{\mu\mu'} \equiv \langle \gamma\mu | V^{\mathrm{SO}} | \gamma'\mu' \rangle = \begin{pmatrix} -\frac{1}{2}\lambda_t & i\sqrt{\frac{3}{2}}\lambda_{te} & 0 \\ -i\sqrt{\frac{3}{2}}\lambda_{et} & 0 & 0 \\ 0 & 0 & \lambda_t \end{pmatrix} \delta_{\mu\mu'}, \qquad \text{(A1)}$$

where $\gamma,\gamma'=\gamma_{8,7t_2},\gamma_{8e}$ and $\lambda_{te}=\langle\gamma_{8t_2}|V^{\rm SO}|\gamma_{8e}\rangle$, which may possibly include a reduction factor. The third term in Eq. (16), which describes the renormalization of the spin-orbit coupling by the covalent hybridization, has a similar structure. It is represented by the matrix

$$M^{\rm SO}_{\gamma\gamma'}\delta_{\mu\mu'}=\begin{pmatrix} -\frac{1}{2}M^{\rm SO}_{t} & i\sqrt{\frac{3}{2}}M^{\rm SO}_{te} & 0\\ -i\sqrt{\frac{3}{2}}M^{\rm SO}_{et} & 0 & 0\\ 0 & 0 & M^{\rm SO}_{t}\end{pmatrix}\delta_{\mu\mu'}, \tag{A2}$$

where $M^{\rm SO}_{te}=\langle\gamma_{8t_2}|W\mathbf{G}V^{\rm SO}|\gamma_{8e}\rangle$. Therefore we can define the matrix of the effective spin-orbit interaction,

$$\widetilde{V}^{\rm SO}_{\gamma\gamma'}\delta_{\mu\mu'}=\begin{pmatrix} -\frac{1}{2}\widetilde{\lambda}_t & i\sqrt{\frac{3}{2}}\widetilde{\lambda}_{te}-M_{te} & 0\\ -i\sqrt{\frac{3}{2}}\widetilde{\lambda}_{et}-M_{te} & 0 & 0\\ 0 & 0 & \widetilde{\lambda}_t\end{pmatrix}\delta_{\mu\mu'}, \tag{A3}$$

in which

$$\widetilde{\lambda}_t=\lambda_t+2M^{\rm SO}_{tt},\quad \widetilde{\lambda}_{te}=\lambda_{te}+2M^{\rm SO}_{te}$$

are effective parameters of the spin-orbit coupling appearing due to the covalent renormalizations of the original parameters λ_t and λ_{te} obtained from the spin-orbit interaction (3). The terms M_{te} are the real parts of the matrix elements $M^{\rm SO}_{\gamma\gamma'}$ and $M^{\rm SO,SO}_{\gamma\gamma'}$ while the $M^{\rm SO,SO}_{\gamma\gamma'}\delta_{\gamma\gamma'}$ terms are neglected.

The situation with the Jahn-Teller interaction is more complicated. The d electron states of the $Cu^{2+}(d^9)$ impurity in a T_d symmetry site can be coupled to the vibrational modes of A_1, E, and T_2 symmetry. Since the excited ^2E state interacts only with the E vibrational mode[32] and the ground $^2T_2$ state is coupled predominantly with the E vibrational modes, we restrict ourselves to consideration of coupling only with the E mode. Then the local distortions of the lattice are described by two normal coordinates Q_u and Q_v of this irreducible representation. As a result the second, Jahn-Teller term in Eq. (16) is

$$V^{\rm JT}_{\gamma\mu\gamma'\mu'}=\left\langle\gamma\mu\left|\frac{\partial V}{\partial Q_u}\right|\gamma'\mu'\right\rangle Q_u+\left\langle\gamma\mu\left|\frac{\partial V}{\partial Q_v}\right|\gamma'\mu'\right\rangle Q_v$$
$$=V_E(\rho^u_{\gamma\mu\gamma'\mu'}Q_u+\rho^v_{\gamma\mu\gamma'\mu'}Q_v). \tag{A4}$$

Now our problem is restricted even more by considering only one mode Q_u. Equation (A4) is rewritten in the form

$$V^{\rm JT}_{\gamma\mu\gamma'\mu'}=V_E\rho^u_{\gamma\mu\gamma'\mu'}Q_u, \tag{A5}$$

which contains the 10×10 matrix

$$\rho^u_{\gamma_{8,7}t\mu\mu'}=\begin{pmatrix}\rho^u_{\gamma_8 e} & \mathbf{0}\\ \mathbf{0} & \rho^u_{\gamma_{8,7}t}\end{pmatrix}, \tag{A6}$$

whose 4×4 block

$$\rho^u_{\gamma_8 e}=\frac{1}{\sqrt{2}}\begin{pmatrix}1&0&0&0\\0&-1&0&0\\0&0&-1&0\\0&0&0&1\end{pmatrix} \tag{A7}$$

is calculated using the four electron basis functions $\{v^-,u^+,u^-,v^+\}$ of the γ_{8e} irreducible representation. The 6×6 block

$$\rho^u_{\gamma_{8,7}t}=\begin{pmatrix}0&0&0&0&\frac{1}{\sqrt{3}}&0\\0&0&0&0&0&-\frac{1}{\sqrt{3}}\\0&0&-\frac{1}{\sqrt{6}}&0&0&0\\0&0&0&-\frac{1}{\sqrt{6}}&0&0\\\frac{1}{\sqrt{3}}&0&0&0&\frac{1}{\sqrt{6}}&0\\0&-\frac{1}{\sqrt{3}}&0&0&0&\frac{1}{\sqrt{6}}\end{pmatrix} \tag{A8}$$

is calculated for six electron functions $\{\gamma_7(\frac{1}{2}),\ \gamma_7(-\frac{1}{2},)\ \gamma_8(-\frac{1}{2}),\ \gamma_8(\frac{1}{2}),\ \gamma_8(-\frac{3}{2}),\ \gamma_8(\frac{3}{2})\}$ of the γ_{7t} and γ_{8t} representations.

Similarly to the case of the spin-orbit coupling, the Jahn-Teller interaction contains a contribution from the hybridization represented by the matrix

$$M^{\rm JT}_{\gamma\gamma'}=2\langle\gamma\mu|WGV^{\rm JT}|\gamma'\mu'\rangle=2M^{\rm JT}\rho^u_{\gamma\mu\gamma'\mu'}Q_u, \tag{A9}$$

whose structure is similar to that of the matrix (A6). As a result the Jahn-Teller interaction has the form

$$\widetilde{V}^{\rm JT}_{\gamma\mu\gamma'\mu'}=\widetilde{V}_E\rho^u_{\gamma\mu\gamma'\mu'}Q_u, \tag{A10}$$

where

$$\widetilde{V}_E=V_E+2M^{\rm JT}$$

is the parameter of the effective Jahn-Teller interaction.

Equation (16) also contains the term $M^{\rm SO,JT}_{\gamma\gamma'}$, mixing the Jahn-Teller and spin-orbit interactions. It has a form of the 10×10 matrix

$$\mathbf{M}^{\mathrm{SO,JT}}=\begin{pmatrix} [\mathbf{M}(\frac{3}{2})] & \mathbf{0} & \mathbf{0} & \mathbf{0} \\ \mathbf{0} & [\mathbf{M}(\frac{1}{2})] & \mathbf{0} & \mathbf{0} \\ \mathbf{0} & \mathbf{0} & [\mathbf{M}(-\frac{1}{2})] & \mathbf{0} \\ \mathbf{0} & \mathbf{0} & \mathbf{0} & [\mathbf{M}(-\frac{3}{2})] \end{pmatrix} Q_u \tag{A11}$$

containing four block matrices, $\mathbf{M}(\mu)$, in its diagonal, with μ being the z components of the total angular momentum **J**. These matrices are

$$\mathbf{M}(-\tfrac{1}{2})=\mathbf{M}(\tfrac{1}{2})=\begin{pmatrix} \frac{1}{\sqrt{6}}M_{\gamma_8 t\gamma_8 t} & -i\frac{\sqrt{3}+1}{2}M_{\gamma_8 t\gamma_8 e} & 0 \\ i\frac{\sqrt{3}+1}{2}M_{\gamma_8 e\gamma_8 t} & 0 & 0 \\ 0 & 0 & 0 \end{pmatrix},$$

$$\mathbf{M}(-\tfrac{3}{2})=\mathbf{M}(\tfrac{3}{2})=\begin{pmatrix} -\frac{1}{\sqrt{6}}M_{\gamma_8 t\gamma_8 t} & i\frac{\sqrt{3}+1}{2}M_{\gamma_8 t\gamma_8 e} \\ -i\frac{\sqrt{3}+1}{2}M_{\gamma_8 e\gamma_8 t} & 0 \end{pmatrix}, \tag{A12}$$

where

$$M_{\gamma\gamma'}=\lambda_{\gamma\gamma''}V^{u}_{\gamma''\gamma}\sum_{\mathbf{k}a}\frac{1}{E-\varepsilon_{\mathbf{k}a}}. \tag{A13}$$

In order to write secular equations we have to calculate the determinant of the 10×10 matrix including all the terms described in this Appendix. Hopefully, the large number of zero elements in this matrix allows us to represent this determinant as a product of the determinants of two 2×2 matrices and of two 3×3 matrices. This allows us to write the secular equations in the form

$$\begin{pmatrix} E-\varepsilon'_{it}(\gamma_8\pm\frac{1}{2}) & \chi_{te}(\gamma_8\pm\frac{1}{2}) \\ \chi^{*}_{et}(\gamma_8\pm\frac{1}{2}) & E-\varepsilon'_{ie}(\gamma_8\pm\frac{1}{2}) \end{pmatrix}=0 \tag{A14}$$

for the basis set $\{\gamma_8 t(\mp\frac{1}{2}),\gamma_8 e(\mp\frac{1}{2})\}$ with the following definitions

$$\varepsilon'_{it}(\gamma_8-\tfrac{1}{2})=\varepsilon'_{it}(\gamma_8\tfrac{1}{2})=\varepsilon_{it}+\tfrac{1}{2}\widetilde{\lambda}_t-\frac{1}{\sqrt{6}}(\widetilde{V}_E+M_{\gamma_8 t_2\gamma_8 t_2})Q_u,$$

$$\varepsilon'_{ie}(\gamma_8-\tfrac{1}{2})=\varepsilon'_{ie}(\gamma_8\tfrac{1}{2})=\varepsilon_{ie}-\frac{1}{\sqrt{2}}\widetilde{V}_E Q_u; \tag{A15}$$

and

$$\begin{pmatrix} E-\varepsilon'_{it}(\gamma_8\frac{3}{2}) & \chi_{te}(\gamma_8\frac{3}{2}) & \frac{1}{\sqrt{3}}\widetilde{V}_E Q_u \\ \chi^{*}_{et}(\gamma_8\frac{3}{2}) & E-\varepsilon'_{ie}(\gamma_8\frac{3}{2}) & 0 \\ \frac{1}{\sqrt{3}}\widetilde{V}_E Q_u & 0 & E-\varepsilon'_{it}(\gamma_7-\frac{1}{2}) \end{pmatrix}=0 \tag{A16}$$

for the basis set $\{\gamma_8 t(\frac{3}{2}),\gamma_8 e(\frac{3}{2}),\gamma_7 t(-\frac{1}{2})\}$ and

$$\begin{pmatrix} E-\varepsilon'_{it}(\gamma_8-\frac{3}{2}) & \chi_{te}(\gamma_8-\frac{3}{2}) & -\frac{1}{\sqrt{3}}\widetilde{V}_E Q_u \\ \chi^{*}_{et}(\gamma_8-\frac{3}{2}) & E-\varepsilon'_{ie}(\gamma_8-\frac{3}{2}) & 0 \\ -\frac{1}{\sqrt{3}}\widetilde{V}_E Q_u & 0 & E-\varepsilon'_{it}(\gamma_7\frac{1}{2}) \end{pmatrix}=0 \tag{A17}$$

for the basis set $\{\gamma_8 t(-\frac{3}{2}),\gamma_8 e(-\frac{3}{2}),\gamma_7 t(\frac{1}{2})\}$ with the definitions

$$\varepsilon'_{it}(\gamma_8\,\tfrac{3}{2})=\varepsilon'_{it}(\gamma_8-\tfrac{3}{2})=\varepsilon_{it}+\tfrac{1}{2}\tilde{\lambda}_t+\frac{1}{\sqrt{6}}(\tilde{V}_E+M_{\gamma_8 t_2\gamma_8 t_2})Q_u\,,$$

$$\varepsilon'_{ie}(\gamma_8\,\tfrac{3}{2})=\varepsilon'_{ie}(\gamma_8-\tfrac{3}{2})=\varepsilon_{ie}+\frac{1}{\sqrt{2}}\tilde{V}_E Q_u\,,$$

$$\varepsilon'_{it}(\gamma_7-\tfrac{1}{2})=\varepsilon'_{it}(\gamma_7\,\tfrac{1}{2})=\varepsilon_{it}-\tilde{\lambda}_t\,, \qquad \text{(A18)}$$

$$\chi_{te}(\gamma_8\mp\tfrac{1}{2})=+i\left(\sqrt{\frac{3}{2}}\tilde{\lambda}_{te}-\frac{\sqrt{3}+1}{2}M_{\gamma_8 t_2\gamma_8 e}Q_u\right)-M_{te}\,,$$

$$\chi_{te}(\gamma_8\mp\tfrac{3}{2})=+i\left(\sqrt{\frac{3}{2}}\tilde{\lambda}_{te}+\frac{\sqrt{3}+1}{2}M_{\gamma_8 t_2\gamma_8 e}Q_u\right)-M_{te}\,. \qquad \text{(A19)}$$

[1] L. D. Landau, Phys. Z. Sowjet **3**, 664 (1933).
[2] E. I. Rashba, Opt. Spectrosc. **2**, 75 (1957); **2**, 90 (1957).
[3] E. I. Rashba and M. D. Sturge, *Excitons* (selected chapter) (North-Holland, Amsterdam, 1987).
[4] Y. Toyozawa, Prog. Theor. Phys. **26**, 29 (1961).
[5] Hitoshi Sumi, J. Phys. Soc. Jpn. **53**, 3498 (1984).
[6] Kagan Yu and K. A. Kikoin, Pis'ma Zh. Éksp. Teor. Fiz. **31**, 367 (1980) [JETP Lett. **31**, 335 (1980)].
[7] B. Volkov and O. Pankratov, Zh. Éksp. Teor. Fiz. **88**, 280 (1985) [Sov. Phys. JETP **61**, 164 (1985)].
[8] V. I. Kaidanov and Yu. I. Ravich, Usp. Fiz. Nauk **145**, 51 (1985) [Sov. Phys. Usp. **28**, 31 (1985)].
[9] A. Abragam and B. Bleaney, *Electron Paramagnetic Resonance of Transition Ions* (Clarendon, Oxford, 1970).
[10] Frank S. Ham, Phys. Rev. **148**, A1727 (1965).
[11] B. Clerjaud and A. Gelineau, Phys. Rev. B **9**, 2832 (1974).
[12] C. A. Bates, Phys. Rep. **35**, 187C (1978).
[13] R. K. Watts, Phys. Rev. **188**, 568 (1969).
[14] Tsuyoshi Yamaguchi and Hiroshi Kamimura, J. Phys. Soc. Jpn. **33**, 953 (1972).
[15] U. Kaufmann, W. H. Koschel, J. Schneider, and J. Weber, Phys. Rev. B **19**, 3343 (1979).
[16] H. Katayama-Yoshida, Int. J. Mod. Phys. **1**, 1207 (1987).
[17] K. A. Kikoin and V. N. Fleurov, *Transition Metal Impurities in Semiconductors. Electronic Structure and Physical Properties* (World Scientific, Singapore, 1994).
[18] C. M. Weinert and U. Scherz, Phys. Status Solidi. B **124**, 287 (1984).
[19] K. A. Kikoin, Fiz. Tverd Tela (Leningrad) **26**, 1933 (1984) [Sov. Phys. Solid State **26**, 1172 (1984)].
[20] C. Bobek, C. Diploma thesis TU Berlin, 1988.
[21] R. Renz and H. J. Shulz, J. Lumin. **24**/**25**, 221 (1981).
[22] I. Broser, R. Broser, and E. Birkicht, J. Lumin. **40**&**41**, 331 (1988).
[23] A. Hoffmann, I. Broser, and P. Thomsen-Schmidt, J. Lumin. **40**&**41** 321 (1988).
[24] P. Dahan and V. Fleurov, Europhys. Lett. **19**, 147 (1992).
[25] P. Dahan and V. Fleurov, J. Phys. Condens. Matter **6**, 101 (1994).
[26] K. A. Kikoin and V. N. Fleurov, J. Phys. C **17**, 2357 (1986).
[27] S. Sugano, Y. Tanabe, and H. Kamimura, *Multiplets of Transition Metal Ions in Crystals* (Academic, New York, 1970).
[28] D. Curie, *Luminescence in Crystals* (Methuen and Co. Ltd., London, 1963).
[29] B. D. Baldassare, *Optical Interactions in Solids* (Wiley, New York, 1968), p. 442.
[30] A. Ismail, Thesis, TU Berlin, 1988.
[31] I. Broser and H.-J. Schulz, J. Electrochem. Soc. **108**, 545 (1961).
[32] B. Clerjaud, A. Gelineau, F. Gendron, C. Porte, J. M. Baranowski, and Z. Liro, J. Phys. C **17**, 3837 (1984).